

# Serrated Structure-Enhanced Microchannel Heat Pipe

LI Qinghua<sup>1</sup>, LI Shuyan<sup>2</sup>, HOU Zhenhua<sup>1,\*</sup>

<sup>1</sup>School of Mechanical and Vehicular Engineering, Changchun University, Changchun 130022, China

<sup>2</sup>Northeast Electric Power University, Jilin 132012, China

\*Corresponding Author Email: HOU Zhenhua

**ABSTRACT:** To explore the mechanism by which the inner wall structure of a heat pipe affects heat dissipation performance, this study innovatively combines the characteristics of a serrated structure with heat pipe technology to design a new type of microchannel heat dissipation structure. Through systematic simulation and numerical analysis methods, the heat dissipation performance and deformation characteristics of this structure under different Reynolds numbers (corresponding to different fluid velocities) are thoroughly investigated. The relationships between structural parameters and heat dissipation performance are analyzed in depth, and the improved model (EHN model) and baseline model (PRO model) are quantitatively compared using temperature as the core evaluation indicator. The results show that the introduction of the serrated structure can significantly enhance microchannel heat dissipation performance. Under  $Re=500$  conditions, the maximum temperature and average temperature of the EHN model are 305.93 K and 304.48 K, respectively, which are 6.71 K and 5.94 K lower than those of the PRO model. The effect of flow velocity on heat dissipation performance shows significant flow regime dependence: in the laminar stage, increasing the inlet flow velocity can rapidly improve heat dissipation performance, while in the turbulent stage, the enhancement effect tends to level off. The serrated structure causes a sharp increase in microchannel pressure drop with increasing Reynolds number; the pressure drop of the EHN model rises steeply from 121.75 Pa at low Reynolds number conditions to 2509.49 Pa at  $Re=3500$ , nearly 19 times higher. From the heat transfer mechanism perspective, the serrated structure increases the effective contact area between the heat dissipation wall and the fluid, providing a more sufficient mass transfer interface for convective heat transfer, thereby enhancing heat transfer efficiency. This study provides theoretical support and data for the structural design and optimization of high-performance microchannel heat sinks.

---

Date of Submission: 13-12-2025

Date of acceptance: 26-12-2025

---

## I. INTRODUCTION

In the field of fluid transport and heat transfer enhancement, the regulation characteristics of the flow field inside the pipeline directly determine the medium transport efficiency, energy loss, and heat transfer performance, and are one of the core issues in the optimal design of industrial systems such as chemical, energy, and HVAC. Although traditional smooth pipes have the advantage of low flow resistance, in scenarios that require enhanced turbulent mixing or increased heat transfer coefficients, their flow field develops too smoothly, making it difficult to meet the engineering demands for efficient heat transfer.

To this end, many researchers have conducted in-depth studies. Various types of microchannels have been investigated, including wavy microchannels [1,2,3], cavity-type microchannels [4,5], and manifold microchannels [6,7], which have been studied in the cooling systems of various devices. For example, Li Yifan et al. designed a periodic fluid disturbance microstructure composed of cavities on the side walls of the microchannel and pin fins in the center of the microchannel. Their study found that the relative length of the bottom of the isosceles trapezoidal cavity (RL) significantly affects the performance of the heat sink. Under low pump power conditions, the overall performance of the heat sink is optimal when  $RL=0.3$ , while under high pump power, the overall performance of the heat sink is best when  $RL=0$  [8]. Meanwhile, other researchers conducted a large number of bionic designs [9,10], finding that they also perform well in heat dissipation. M et al. found that when the total lengths of the evaporator, adiabatic, and condenser sections of a heat pipe are 300 mm with a 1:1:1 ratio, the wall temperature is reduced by 11.9%, the thermal resistance decreases, and the heat transfer coefficient is increased by 85.68% compared to a uniform geometry heat pipe [11]. Wang et al. studied and compared shark skin texture, fish scale texture, and crab surface texture for heat dissipation performance, and found that among the three bionic textures, the bionic crab shell texture exhibited the best heat dissipation [12].

This article introduces artificial structured surfaces on the inner wall of pipelines, using wall morphology to disturb the boundary layer, thereby altering the flow state and energy distribution of the fluid. Among them, sawtooth-shaped structures, due to their flexible geometric parameters and relatively simple manufacturing processes, can also change the direction of fluid flow, induce vortex generation, and enhance boundary layer separation and reattachment, making them an important means to regulate pipeline flow characteristics.

Parameters such as the tooth height, tooth width, tooth angle, and arrangement of the sawtooth structure directly affect the distribution of turbulence intensity in the flow field, the scale and evolution of vortices, and consequently have a significant impact on flow resistance coefficients, local pressure losses, and heat transfer efficiency. In-depth exploration of the influence mechanism of sawtooth shapes on the pipeline flow field can not only reveal the interaction rules between structured walls and fluids but also provide a theoretical basis for the design and optimization of high-efficiency, low-consumption pipeline components, holding important engineering value and practical significance for promoting energy-saving, consumption-reducing, and performance-enhancing in industrial fluid systems.

## II. Information and methodology

### Nondimensionalization of the hydrodynamic equations.

The flow of fluid within the intercooler follows the conservation of mass, momentum, and energy.

$$\begin{cases} \text{Continuity equation: } \frac{\partial \rho}{\partial t} + \nabla(\rho v) = 0 \\ \text{Momentum conservation equation: } \rho \frac{dv}{dt} - \rho F - \text{div} P = 0 \\ \text{Energy conservation equation: } \rho c_p \frac{\partial T}{\partial t} + \rho c_p (V \nabla) T = \frac{D_p}{D_t} + \nabla(k \nabla T) + \Phi \end{cases} \quad (1)$$

In equation (1):  $h$  is the specific enthalpy of the fluid,  $\rho F$  represents the body force per unit volume,  $\lambda$  is the thermal conductivity,  $\Phi$  is the heat source within the fluid,  $\text{div} P$  represents the divergence of the stress tensor per unit volume, and  $\Phi$  is the dissipation function.

Non-dimensionalizing the mass conservation equation yields equation (2):

$$\left( \frac{L_0}{t_0 U_0} \right) \frac{\partial \rho^*}{\partial t^*} + \nabla^* \cdot (\rho^* V^*) = 0 \quad (2)$$

Non-dimensionalizing the momentum conservation equation yields equation (3):

$$\frac{L_0}{U_0 t_0} \frac{\partial (\rho^* V^*)}{\partial t^*} + \nabla^* \cdot (\rho^* V^* V^*) = \frac{g_0 L_0}{U_0^2} \rho^* f^* - \frac{P_0}{\rho_0 U_0^2} \nabla p^* + \frac{\mu_0}{\rho_0 U_0 L_0} \nabla \tau^* \quad (3)$$

Non-dimensionalizing the energy conservation equation yields equation (4):

$$\frac{L_0}{t_0 U_0} c_p^* p^* \frac{\partial T^*}{\partial t^*} + c_p^* p^* (V^* \nabla^*) T^* = \frac{\mu_0}{\rho_0 U_0 L_0} \frac{k_0}{c_p u_0} \nabla^* \cdot (k^* \nabla^* T^*) + \frac{L_0}{U_0 T_0} \frac{P_0}{\rho_0 c_p T_0} \frac{D p^*}{D t} + \frac{\mu_0 U_0^2}{\rho_0 U_0 L_0 c_p T} \phi^* \quad (4)$$

### Reynolds number

The Reynolds number is a dimensionless quantity used to characterize the state of a fluid, given by equation (5)

$$\text{Re} = \frac{\rho \bar{v} d}{\mu} \quad (5)$$

In equation (5):  $\rho$  is the density of the working medium,  $\bar{v}$  is the average velocity of the working medium,  $d$  is the characteristic length of the working channel,  $\mu$  is the viscosity coefficient of the working medium.

### Model Building

To investigate the effect of serrated structures on the heat dissipation performance of heat pipes, this study constructed two comparative models composed of a fluid domain and the heat pipe body (see Figure 1 (a) and (b)), defined as the PRO model and the EHN model, respectively. The PRO model is a conventional heat pipe model with an unmodified structure; the improved EHN model is based on the PRO model, with regularly arranged serrated protrusions on the inner wall of the heat pipe. The total length ( $L_1$ ) of both models is 100 mm, the outer diameter ( $D_1$ ) is 20 mm, and the inner diameter ( $D_2$ ) is 15 mm. For the EHN model, the serrated features have a length ( $L_1$ ) of 4 mm and a width ( $L_2$ ) of 2 mm, as shown in Figures 1(c) and (d).

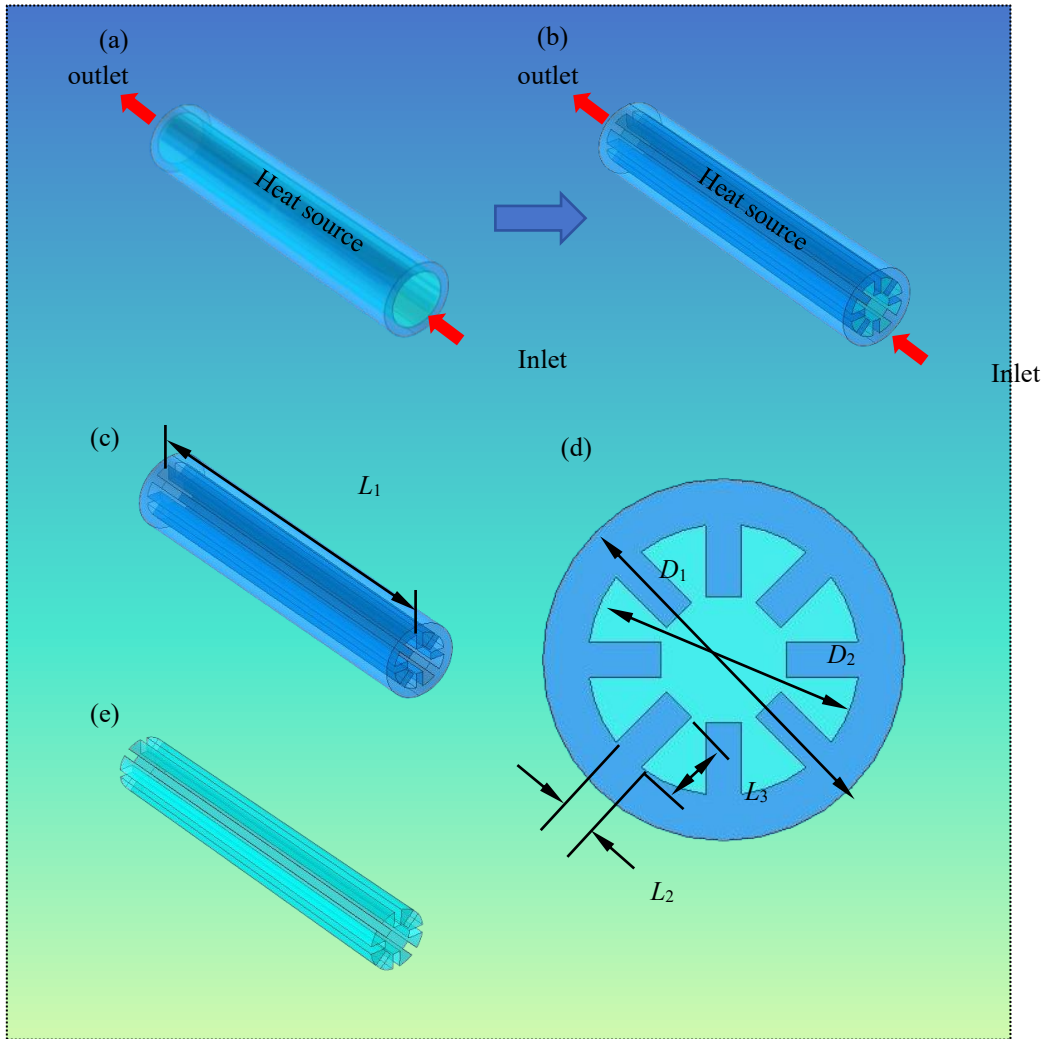


Fig. 1 Model construction. (a) Traditional model PRO; (b) Improved model EHN; (c) Heat pipe part of the EHN model; (d) Cross-section of the EHN model; (e) Fluid domain model of the EHN model.

### Grid Validity Verification

This study uses a multi-region meshing method to divide the model into two core parts: the heat transfer module and the flow channel section. To ensure the accuracy of simulation calculations, the grid division in the flow channel section is finer than that in the solid section, and both sections uniformly use tetrahedral mesh division. An expanded mesh is added to the boundary layer between the heat transfer module and the flow channel section, with five layers. The number of mesh elements in each region is as follows: 9,397,157; 1,577,045; 297,473; 107,478; 60,713; 33,084; 26,432. A series of simulation experiments show that when the number of mesh elements exceeds 1,577,045, the fluctuation amplitude of pressure drop tends to stabilize (see Figure 2). This result indicates that to ensure the validity of the mesh division and the accuracy of the simulation data, the number of mesh elements should not be less than 1,577,045.

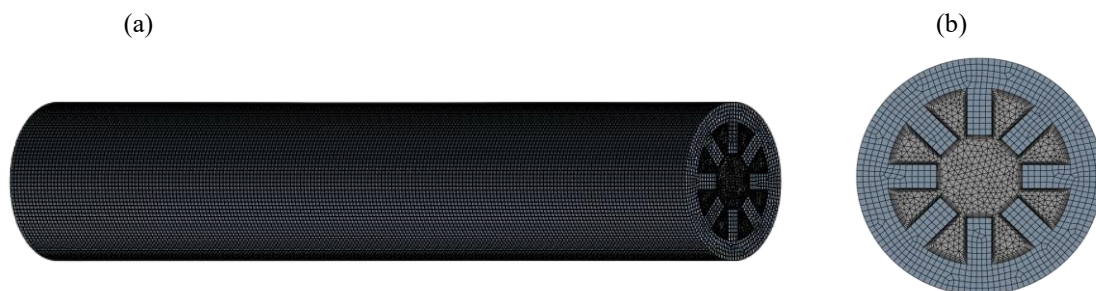


Fig. 2 Mesh Division. (a) Overall Mesh Division; (b) Section Mesh Division

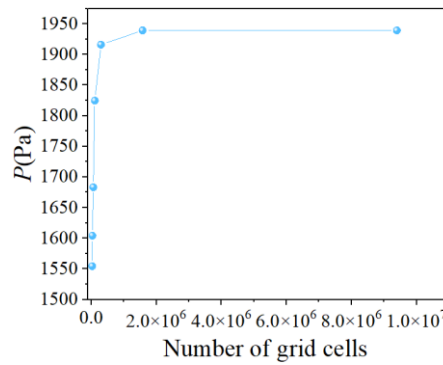


Fig. 3 Grid Verification

### III. RESULTS AND DISCUSSION

To investigate the impact of the inner wall structure of heat pipes on their heat dissipation performance, this study systematically analyzed the relationship between structural parameters and heat dissipation performance through differentiated design of the heat pipe inner wall. In the quantitative comparison of heat dissipation performance, temperature is the most intuitive core evaluation metric. The results show that, whether under laminar or turbulent flow conditions, the heat dissipation performance of the EHN model is significantly better than that of the traditional PRO model.

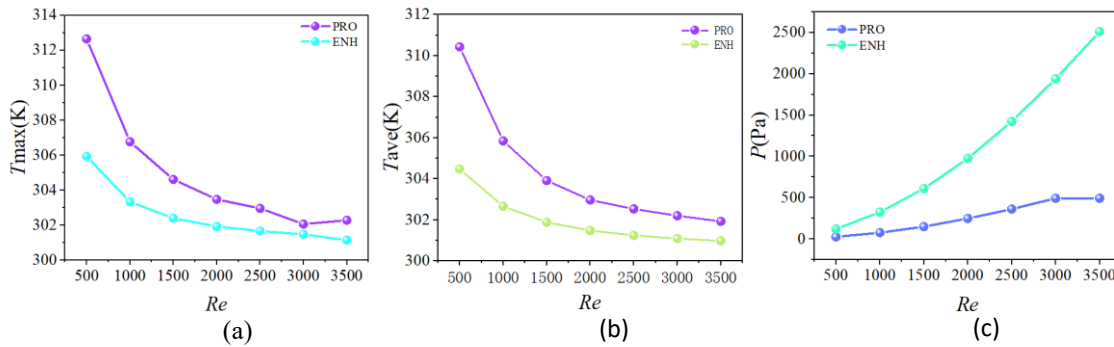


Fig.4 Heat dissipation evaluation indicators. (a) Maximum temperature of the heat dissipation surface, (b) Average temperature of the heat dissipation surface, (c) Pressure drop

Figures 4(a) and 4(b) respectively present the variation patterns of the maximum and average temperatures on the heated surface for the two models. In the laminar flow regime, the initial maximum temperature of the PRO model is 312.65 K. As the Reynolds number ( $Re$ ) increases, its temperature exhibits a sharp decreasing trend: when  $Re$  rises from 500 to the critical value for turbulence, the maximum temperature on the heat-dissipating surface drops to 303.48 K, and the average temperature decreases from 310.43 K to 302.97 K. Correspondingly, for the EHN model, the maximum temperature decreases from the initial 305.93 K to 301.93 K, and the average temperature drops from 304.48 K to 300.80 K. Comparatively, the maximum temperature of the EHN model is 6.72~1.55 K lower than that of the PRO model, and the average temperature is 0.014~0.219 K lower. Upon entering the turbulent regime, the temperature decrease rate for both models significantly slows down. When  $Re$  increases from 2000 to 3500, the maximum temperature of the PRO model's heat-dissipating surface decreases by only 1.2 K, and the average temperature decreases by 1.044 K; for the EHN model, the maximum and average temperatures decrease by 0.784 K and 0.500 K, respectively.

The fundamental reason for this performance difference lies in the introduction of the serrated feature: under the given spatial constraints, the alternate concave-convex serrated structure of the inner wall significantly increases the effective contact area between the heat-dissipating wall and the fluid. The larger contact area provides a sufficient interface for convective heat transfer, enabling the fluid to absorb heat from the wall more effectively as it flows through the channel, thereby significantly enhancing the overall heat dissipation efficiency, as shown in Figure 5.

However, it should be noted that the embedding of serrated features inevitably compresses the effective flow cross-sectional area of the channel. According to the fluid mechanics continuity equation and Bernoulli's principle, when fluid flows at a constant rate in a closed channel, a reduction in the cross-sectional area directly leads to an increase in flow velocity; at the same time, an increase in the complexity of the wall structure significantly increases both local and frictional resistance in the channel. The superposition of these two factors

ultimately results in a significant rise in pressure drop within the channel. As shown in Figure 4(c), the pressure drop of the EHN model rises from the initial 121.747 Pa to 2509.49 Pa, an increase of over 19 times, far higher than that of the PRO model under the same conditions.

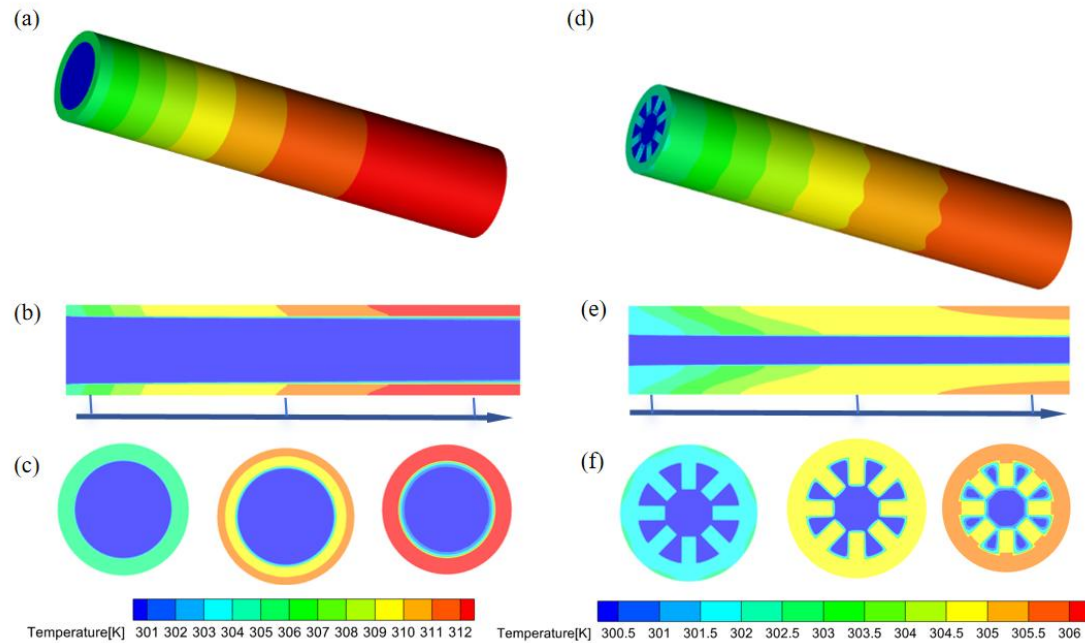


Fig.5 Heat pipe temperature cloud map. (a) Temperature cloud map of the PRO model; (b) Longitudinal section temperature cloud map of the PRO model; (c) Transverse section temperature cloud map of the PRO model; (d) Temperature cloud map of the EHN model; (e) Longitudinal section temperature cloud map of the EHN model; (f) Transverse section temperature cloud map of the EHN model

#### IV. CONCLUSION

This paper innovatively combines the characteristics of a serrated structure with heat pipe technology to design a novel microchannel cooling structure. Systematic simulations and numerical analyses were conducted on the thermal performance and deformation characteristics of this structure, with an in-depth investigation into how different Reynolds numbers (corresponding to different fluid velocities) affect its thermal performance and deformation characteristics. Based on the combined results of simulations and numerical analyses, the main conclusions of this study are as follows:

(1) The introduction of a serrated structure significantly enhances the thermal performance of the microchannel. Under the condition of Reynolds number  $Re=500$ , the maximum and average temperatures of the baseline model (PRO model) are 312.64 K and 310.427 K, respectively; while in the improved model with the serrated structure (EHN model), the maximum temperature drops to 305.93 K and the average temperature drops to 304.48 K. Compared with the baseline model, the maximum temperature of the improved model decreases by 6.71 K, and the average temperature decreases by 5.94 K, indicating a significant improvement in cooling performance.

(2) The enhancement effect of fluid velocity on thermal performance exhibits a clear dependence on the flow regime. In the laminar flow stage, increasing the inlet velocity can rapidly improve the thermal performance; however, in the turbulent flow stage, further increasing the inlet velocity yields diminishing gains in thermal performance. Quantitative analysis shows that in the laminar stage, the maximum temperature of the baseline model decreases by as much as 9.17 K, and the average temperature decreases by 0.85 K; whereas in the turbulent stage, the maximum temperature decreases by only 1.19 K, and the average temperature decreases by just 0.09 K.

(3) Introducing the serrated structure causes the pressure drop across the microchannel to rise sharply with increasing Reynolds number. Numerical calculations indicate that the initial pressure drop of the improved model (EHN model) under low Reynolds number conditions is only 121.75 Pa; when the Reynolds number rises to 3500, the pressure drop surges to 2509.49 Pa, nearly 19 times higher than the initial condition, highlighting the significant influence of the serrated structure on flow resistance.

## REFERENCES

- [1]. Ji-Feng Zhu, Xian-Yang Li, Shuo-Lin Wang, Yan-Ru Yang, Xiao-Dong Wang, Performance comparison of wavy microchannel heat sinks with wavy bottom rib and side rib designs, *International Journal of Thermal Sciences*, 2019, 146:106068.
- [2]. Shuo-Lin Wang, Ji-Feng Zhu, Di An, Ben-Xi Zhang, Liu-Yi Chen, Yan-Ru Yang, Shao-Fei Zheng, Xiao-Dong Wang, Heat transfer enhancement of symmetric and parallel wavy microchannel heat sinks with secondary branch design, *International Journal of Thermal Sciences*, 2022, 171:107229.
- [3]. Shuo-Lin Wang, Di An, Yan-Ru Yang, Shao-Fei Zheng, Xiao-Dong Wang, Duu-Jong Lee, Heat transfer and flow characteristics in symmetric and parallel wavy microchannel heat sinks with porous ribs, *International Journal of Thermal Sciences*, 2023, 1185:08080.
- [4]. Shaoxi Wang, Shenxin Yu, Weiting Chen, Yu Wang, Antong Bi, Zeyang An, Yue Diao, Wei Li, Yucheng Wang, Study on microfluidic heat dissipation enhancement and thermal stress analysis in three-dimensional integrated circuit with through silicon via structures, *Applied Thermal Engineering*, 2025, 279:127699.
- [5]. Huang Binghuan, Mi Chuang, Li Kui, et al. Investigation of Flow and Heat Transfer Characteristics for Fins Compound with Cavities in Microchannels[J]. *Journal of Refrigeration*, 2023, 44(4).
- [6]. Wu, Z., Xiao, W., He, H. et al. Jet-enhanced manifold microchannels for cooling electronics up to a heat flux of 3,000 W cm<sup>-2</sup>. *Nat Electron*, 2025, 8:810 – 817
- [7]. Luo, Y., & Li, W. Simulation of subcooled flow boiling in manifold microchannel heat sink. *Numerical Heat Transfer, Part A: Applications*, 2020, 77(11): 951 – 965.
- [8]. Zhang Qiankun, Li Hongyan, Lü Bichun, et al. Numerical Study of Thermal-Hydraulic Characteristics of Vein Biomimetic Microchannel Heat Exchanger[J]. *Journal of Refrigeration*, 2025, 46(4): 52-60.
- [9]. Zhang, Yixuan, Deyuan Zhang, Dongyue Wang, and Xiangyu Zhang. "Study on the Heat Reduction Effect of Biomimetic Unidirectional Transporting Channels Inspired by *Nepenthes alata*" *Biomimetics* 4, no. 2019, 4: 70.
- [10]. Lihang Yu, Binbin Jiao, Yuxin Ye, Xiangbin Du, Yanmei Kong, Ruiwen Liu, Jingping Qiao, Shichang Yun, Zhiqiang Wang, Wei Li, Yingzhan Yan, Dichen Lu, Ziyu Liu, Ronggui Yang, An adaptive thermal management method via bionic sweat pores on electronic devices, *Applied Thermal Engineering*, 2024, 247, 122953.
- [11]. M. Sakthi Priya, D. Sakthivadivel, Performance assessment of a geometrical modification on thermosyphon heat pipe with the assistance of novel convergent-divergent truncated cones for energy recovery systems, *Applied Thermal Engineering*, 2024, 247:122999.
- [12]. Jin Wang, Jin Yao, Xuan Liang, Zhenxin Li, Fei Lu, Lidija Čuček, Dan Zheng, Numerical investigation on thermal – hydraulic performance of an intercooler with bionic channel textures, *International Journal of Heat and Fluid Flow*, 2025, 112:109744.